Tracing the geomagnetic field intensity variations in Upper Mesopotamia during the Pottery Neolithic to improve ceramic-based chronologies

Y. Gallet[1], A. Fournier[1], P. W. Livermore[2]

[1]*Université de Paris, Institut de Physique du Globe de Paris, CNRS, F-75005 Paris, France*

[2]*School of Earth & Environment, University of Leeds, Leeds LS2 9JT, UK*

Abstract

The transdimensional Bayesian method AH-RJMCMC applied to archeomagnetic intensity data available in the Balkans and the Near East allows us to estimate the variations in intensity of the geomagnetic field in Upper Mesopotamia during the 7th and 6th millennia BCE (Late Neolithic), with adequate treatment of the dating and intensity uncertainties. The results for the 6th millennium BCE appear particularly interesting because there is enough data to trace rapid geomagnetic field intensity variations, with two century-scale peaks around 5800 BCE and 5550 BCE, associated with rates of changes (>0.2 μT/year) higher than the maximum rate observed in the current geomagnetic field. We show that these variations could help decipher the correlations between different archeological sequences or periodizations established from scattered sites in Upper Mesopotamia. So far documented only from the Balkan data, the intensity peak occurring around 5800 BCE may provide accurate chronological constraints for the Early Halaf phase. New insights are also obtained for the Halaf-Ubaid Transitional phase (end of the 6th millennium BCE), which remains poorly defined from an archeological point of view. The AH-RJMCMC results imply that either the archeointensity data currently available from Upper Mesopotamia document only the beginning of this phase, or that this phase occurred between ~5400 and ~5200 BCE, shorter

than often considered. Such preliminary archeological inferences will progress and broaden with the addition of new archeointensity data.

Keywords: archeomagnetic intensity variation, transdimensional Bayesian method, pottery horizons, Late Neolithic, archeological inferences

1. Introduction

The end of the Neolithic in the Near East was a period of profound cultural and social transformations probably linked, at least in part, to the definitive adoption of pottery around 7000 BCE and then to its wide regional diffusion and diversification, with technological improvements, throughout the 7th and 6th millennia BCE (e.g. Akkermans and Schwartz, 2003; Nieuwenhuyse et al., 2010; 2013; Tsuneki et al. 2017; Gómez-Bach et al., 2018a; Nieuwenhuyse, 2018a,b). As early as the period known as the Pottery Neolithic or Late Neolithic, ceramic horizons are therefore of great importance for establishing a regional periodization valid for scattered archeological sites, especially in Syria and Iraq, and/or for synchronizing occupation phases between different agricultural settlements in Upper Mesopotamia whose number increased considerably during the 7th and 6th millennia BCE (e.g. Akkermans and Schwartz, 2003; Huot, 2004).

Many questions remain with regard to the meaning and interpretation, in terms of chronological constraints, of the stylistic differences (vessel shapes and decorations) observed between ceramics found in Neolithic sites scattered across Upper Mesopotamia. They are all the more significant as the degree of standardization of ceramic production remains poorly understood for this ancient period, the very notion of regional standardization not even being assured (see the discussions by Hole (2013), Frangipane (2013) and Nieuwenhuyse (2013)). To briefly summarize, it is indeed particularly difficult to disentangle a difference of essentially local origin (what Hole (2013) compared to dialect variations in language), possibly associated with a lack of social interaction, rejection or different conservatism between villages, from a difference of broader origin that could reflect changes of techniques and/or preferences, for example through artistic emulation between settlements (recall the beauty and sophistication of the decorations on ceramics from the so-called Halaf period during the 6th millennium BCE; e.g. Akkermans and Schwartz, 2003; Nieuwenhuyse et al., 2013 and references therein). This last option would allow for a regional network of social interactions to be envisaged. Such interactions may have taken the form of trade (e.g. Davidson and McKerrell, 1980; Davidson, 1981; Spataro and Fletcher, 2010), the pottery being a commercial product par excellence, surplus exchanges (Gómez-Bach et al., 2018b), or they may have been associated with the displacement of artisan potters throughout Upper Mesopotamia. Furthermore, the possibility that women played a role in the dissemination of pottery know-how through marriages between people from different localities cannot be ruled out (e.g. Robert, 2010; Forest, 2013).

Dates are crucial here, especially since the history of archeological discoveries and regional geopolitical vicissitudes have led to archeological chronologies with different terminologies established between the east and west of Upper Mesopotamia since the 1930s (e.g. Nieuwenhuyse et al., 2013 and references therein). Nowadays it is very difficult to accurately synchronize these chronologies due to the lack of sufficient radiocarbon dating in many sites, as well as sometimes to the lack of precise description of the ceramic typologies and/or of the archeological contexts in which the pottery was discovered more than half a century ago (a synthesis of available data is provided by Nieuwenhuyse et al. (2013), Nieuwenhuyse (2018a), Gómez-Bach et al. (2018a) and references therein).

This study aims to enable progress in the study of chronologies, by demonstrating the importance of using variations in geomagnetic intensities as chronological markers. Recent studies have shown the potential of archeomagnetism for archeological practice, in particular for dating burnt structures found in situ (such as pottery or domestic kilns) and the associated archeological contexts. For the most part, they focused on structures dated from the past two millennia, the archeomagnetic dating relying mainly on the directional geomagnetic field variations (e.g. Gallet et al., 2009; Principe et al., 2018; Korte et al., 2019; Genevey et al., 2021). Thanks to the recent acquisition of numerous new data on geomagnetic field intensities, particularly in the Near East, archeointensities can now also be used to provide chronological constraints, opening a wide field of investigation on ceramic productions (i.e. materials found displaced from the place where they were fired and therefore for which all information from geomagnetic directions is lost; e.g. Genevey et al., 2021). The technique used for this purpose can either rely on a statistical correlation between a result of unknown age and a reference (dated) geomagnetic secular variation curve (e.g. Le Goff et al., 2002; Pavón-Carrasco et al., 2011) or on posterior probability distributions of age values determined by marginalization from a Bayesian approach (e.g. Schnepp et al., 2015; Hervé and Lanos, 2017; Livermore et al., 2018) (see further discussion and comparison between the two methods in Genevey et al., 2021). It should be noted that dating based on a single archeointensity value can lead to poorly constrained results, especially if analyzed in the absence of other archeological, archeomagnetic (i.e. direction-based) or isotopic (radiocarbon) information. However, two studies focusing on time-ordered series of results dated to the 3rd and 2nd millennia BCE in the Near East recently illustrated the contribution of archeointensity alone to archeomagnetic dating (Gallet et al., 2020; Shaar et al., 2020). They both rely on the recent development of a new transdimensional Bayesian technique allowing the construction of regional geomagnetic intensity variation curves, not based on any a priori assumption as to the nature of the geomagnetic variations sought (Livermore et al., 2018; 2021). This method makes it possible to trace fluctuations of highly variable nature both in amplitude and duration (from a few decades to several millennia), without the need to seek a compromise through a global regularization parameter that smoothes the entire model. The main objective of our study is to apply this method to the archeomagnetic intensity results obtained in the Balkans dating from the 6th millennium BCE (Kovacheva et al., 2014; Kostadinova-Avramova et al., 2019), to the data from the 7th and 6th millennia BCE currently available in the Near East (Gallet et al., 2015; Yutsis-Akimova et al., 2018a, 2018b), and finally, to construct a composite Upper Mesopotamian archeointensity variation curve between 7000 BCE and 5000 BCE, with adequate treatment of the dating and intensity uncertainties, assuming that the Balkans and Upper Mesopotamia shared the same secular variation in geomagnetic field intensity during this time interval.

At this stage, our study is intended to illustrate the potential of a method that could later integrate new archeological contexts, with pottery fragments already available in archeological repositories or still to be discovered in the Near East. In addition to the information on the behavior of the geomagnetic field during the 7th and 6th millennia BCE, the results already obtained bring new perspectives to refine the archeological chronologies of the Pottery Neolithic period in the Near East.

2. Selected datasets and methodology

2.a Archeointensity datasets

For the Balkans, the results dating from the 6th millennium BCE were obtained in the Paleomagnetism laboratory of Sofia (Bulgaria) under the direction of M. Kovacheva. Mainly deriving from in-situ burnt structures, the Bulgarian dataset was compiled by Kovacheva et al. (2014). More recently, new archeointensity data were obtained by Kostadinova-Avramova et al. (2019), which have therefore also been taken into account in the present work. To these data, a result obtained in Northern Greece by Fanjat et al. (2013) was also added. In total, the database compiled for the Balkans contains 51 archeointensity values whose dating is based on archeological constraints and/or radiocarbon data (Table S1; more information is available in the associated articles). For simplicity, given the lack of precise information on the probability distributions of radiocarbon dates, we considered below only uniformly distributed age uncertainties. Furthermore, a time-order relationship was applied for a few limited sets of data (Table S1).

The Upper Mesopotamian data were obtained from groups of pottery fragments sampled in Syria, at Tell Halula (e.g. Molist et al., 2013) and Tell Masaikh (Robert, 2010), and in Northern Iraq, at Yarim Tepe I and II (e.g. Merpert and Munchaev, 1987, 1993a,b; Amirov, 1994; 2018). In all cases, these are multi-layered sites that have been the subject of detailed excavations. Each group, which includes a minimum of three fragments from different pottery that gave intensity values satisfying a set of selection criteria using the Triaxe experimental protocol (e.g. Le Goff and Gallet, 2004; Gallet and Le Goff, 2006; Gallet et al., 2020), is directly associated with an archeological level, itself placed in a stratigraphic/temporal sequence. Here we consider the ceramic (chronological) phasing as provided by the archeologists. At Tell Halula, 22 groups of potsherds gave archeointensity values spanning the 7th and 6th millennia BCE, i.e. during the so-called Initial Pottery Neolithic, Early Pottery Neolithic, pre Halaf, proto-Halaf and Halaf cultural phases (Molist et al., 2013; Gallet et al., 2015; Nieuwenhuyse et al., 2013; Nieuwenhuyse, 2018a). However, the last centuries of the 6th millennium corresponding to the so-called Halaf Ubaid Transitional (HUT) period are not represented in this site, which is instead likely represented at Tell Masaikh with two archeointensity values (Robert et al., 2008; Robert, 2010; Gallet et al., 2015). It is nevertheless important to emphasize the great archeological uncertainties that remain concerning the definition, or even the existence, of the HUT phase (e.g. Campbell, 2007;

Campbell and Fletcher, 2010; Gómez-Bach et al., 2016; Nieuwenhuyse et al., 2016). The Iraqi sites of Yarim Tepe II and I excavated by Soviet archeologists in the 1970s yielded respectively 23 and 9 archeointensity values, from nine and eight different archeological levels (or building horizons). At Yarim Tepe II, the temporal sequence with intensity data ranges from the end of the Early Halaf / beginning of the Middle Halaf to the HUT period (e.g. Amirov, 1994; 2018; Yutsis-Akimova et al., 2018a), while that of Yarim Tepe I partially covers the archaic Hassuna and the standard Hassuna phases dated from the end of the 7th millennium and beginning of the 6th millennium BCE (e.g. Bashilov et al., 1980; Bader, 1989; Bernbeck and Nieuwenhuyse, 2013; see also Yutsis-Akimova et al., 2018b). To all these data is added a new Triaxe archeointensity result obtained from a group of potsherds sampled at Tell Begum in Iraqi Kurdistan, dated archeologically and by radiocarbon from the HUT period around 5400 BCE (Fig. S1; Table S2; Nieuwenhuyse et al., 2016; Nieuwenhuyse, 2018; Odaka et al., 2019). In total, the Near-Eastern archeointensity database contains 57 values (Table S1). Uniformly distributed age uncertainties were considered for all these data.

2.b Outline of the transdimensional Bayesian method AH-RJMCMC

The transdimensional Bayesian method AH-RJMCMC (Age Hyperparameter Reverse Jump Monte Carlo Markov Chain) was developed by Livermore et al. (2018) to model regional geomagnetic field intensities. The detailed description of this approach is provided in the 2018 publication, and only the main points are outlined below. An ensemble of piecewise linear fits to the data are calculated, whose statistics converge to those of the posterior probability distribution of the intensity variation given the dataset. Each member of the ensemble comprises a series of linear segments whose number, which defines the complexity of the underlying geomagnetic variations, is determined by the data themselves according to their dating and experimental uncertainties. AH (from AH-RJMCMC) means that the ages of the data are themselves introduced into the model vector, which makes it possible to take into account, in addition to the uncertainties on dating, possible temporal relationships existing between certain data or certain datasets (Livermore et al., 2018; Gallet et al., 2020; Shaar et al., 2020). This is a crucial element when analyzing the Near-Eastern data obtained from multi-layered archeological sites. The output is dependent on the prior information adopted, which includes a maximum number of linear segments, set here to 150, large compared to the 2000 years of the time interval considered (~7000-5000 BCE), and minimum and maximum values of the intensity of each interior vertex, set respectively to 20 μT and 70 μT. An ensemble size of 200 million individual models, large enough to ensure convergence, is computed following a perturbation scheme, using a Monte Carlo Markov chain algorithm, applied to the number of segments (with the addition or removal of a segment), the age and intensity of the knots and the data ages. Note that no form of weighting between the data, other than that introduced by their experimental and age uncertainties, was implemented for these calculations.

The AH-RJMCMC algorithm provides a probability density distribution as a function of time for geomagnetic field intensity, for which the average, median, mode and 95% credible interval are determined. Although each individual model is piecewise linear, these diagnostics over the whole ensemble are smooth curves. By marginalization, it is also possible to determine the posterior probability distributions of the age and intensity of each datum, which indicate their most probable values given the characteristics (number, temporal distribution and uncertainties) of the dataset available during the age interval studied. Finally, it should be noted that an important advantage of this method lies in the absence of an ad-hoc regularization parameter and that it therefore allows variations with very different timescales to be determined, if these are actually required by the data. Such a characteristic is particularly valuable for identifying rapid variations as seems to be the case in the 6th millennium BCE (Livermore et al., 2018; 2021; Yutsis-Akimova et al., 2018a,b).

3. Modeling results

3.a Balkans (6th millennium BCE.)

The evolution of the geomagnetic field intensity obtained in the Balkans from the AH-RJMCMC method is shown in Fig. 1a (Table S3; note that all data were transferred to the latitude of Sofia, Bulgaria). The median values of the intensity probability distribution are reported because this indicator is less sensitive than the average to the extreme values given by some of the model ensemble. This evolution, similar to that proposed by Kovacheva et al (2014) using the Bayesian method developed by Lanos (2004) (pale-orange area in Fig. 1a), is marked by two intensity peaks of ~200 years duration, the most recent with a maximum around 5555 BCE, the oldest with its maximum around 5805 BCE. The latter is still rather poorly defined due to the small number of data (two) available for the first two centuries of the 6th millennium BC; this translates into a large credible interval during this period. The minimum of geomagnetic intensities during the 6th millennium occurs around 5400 BCE and is followed by a steady increase in intensities until the end of the millennium.

The median intensity values range from ~30 μT to more than 60 μT throughout the 6th millennium BCE (Fig. 1a), suggesting rapid fluctuations. This is attested by the calculation of the variation rates (time derivative of the median intensity curve) shown in Fig. 1b (Table S3). The two intensity peaks mentioned above are associated with maximum rates of change of the order of ~0.27 μT/year. This value is significantly higher than that mentioned by Kostadinova-Avramova et al. (2019), with a value of ~0.11 μT/year estimated for the peak centered around 5550 BCE. This difference is related to both the different databases and characteristics of the two methods used for the calculation of geomagnetic evolutions (Lanos, 2004; Livermore et al., 2018), in particular with the absence of any regularization applied in the AH-RJMCMC method.

The data reported in Kovacheva et al (2014) were obtained over many years, and they do not all share the same experimental criteria. In order to assess at first order the sensitivity of the evolution described above to these experimental differences, the Balkan database was subdivided according to whether or not the intensity determinations included pTRM checks (Thellier and Thellier, 1959). When pTRM checks were carried out at least partially, i.e. for the most recent data, the experimental uncertainties of the intensity values were kept as published (circles in Figs. 1a and S2a,c). Conversely, when the data were not constrained by pTRM checks, their experimental uncertainties have been arbitrarily set to 5 μT when the published ones are below this threshold (otherwise they have been kept as published; blue triangles in Figs. 1a and S2a,c; Table S1). In addition, we roughly and arbitrarily considered that the temporal uncertainties of the data could not be less than ±50 years. The variations in geomagnetic field intensity calculated from this modified dataset are shown in Fig. S2a (Table S3). These are very close to those exhibited in Fig. 1a, with two intensity peaks still well expressed. This is also the case when the minimum temporal uncertainty is set to ±75 years (Fig. S2c; Tables S1, S3). The maximum rates of change associated with the intensity peaks also remain of the order of 0.20-0.25 μT/year (Fig. S2b,d). The variations shown in Fig. 1a thus appear reasonably robust, even if the acquisition of new archeointensity data appears to be still necessary, especially for the beginning of the 6th millennium BCE.

3.b Upper Mesopotamia (7th-6th millennium BCE)

The archeointensity results available in the Near East have been dated according to the typo-morphology of ceramics and by some radiocarbon data (Bernbeck and Nieuwenhuyse, 2013; Molist et al., 2013; Yutsis-Akimova et al., 2018a,b; Nieuwenhuyse, 2018a, Gómez-Bach et al., 2018a and references therein). Here we adopt a cautious approach that emphasizes the link of the groups of potsherds with archeological periods (such as Middle Halaf or Late Halaf) and the fact that these fragment groups are all associated with well-recognized archeological levels, with time order relationships between them in the different sites. On the other hand, the constraints provided by the relative thicknesses of the stratigraphic layers identified at Yarim Tepe II and I (see in Yutsis-Akimova et al., 2018a,b) are ignored because these thicknesses vary laterally on the surface of the sites and so certain stratigraphic layers may have been partially or completely leveled, which casts some doubt on their relevance. Neglecting the relative thicknesses of the layers also avoids the need for a priori knowledge on the evolution of accumulation rates across these sequences. Hence, for these two sites, temporal relationships were only considered between the different archeological levels defined by the archeologists. This means that any subset of archeointensity data within a level is not ordered in time (regardless of their stratigraphic position), but nevertheless must have an age, which is (respectively) greater or younger than those data in levels immediately above or below. This approach also places much less emphasis on individual dating of data (a radiocarbon-dated bone fragment may have moved within a stratigraphic sequence; e.g. Yutsis-Akimova et al., 2018b). It is thus very different from that previously used by Yutsis-Akimova et al. (2018a,b).

The archeological periodization used and the associated dates are essentially those given by Molist et al (2013) (see more discussion in Bernbeck and Nieuwenhuyse, 2013) and Nieuwenhuyse (2018a). For the cultural phases preceding the Halaf (Initial Pottery Neolithic, Early Pottery Neolithic, pre Halaf, proto-Halaf), the dating of the archeological transitions relies primarily on the large set of radiocarbon dates obtained at Tell Sabi Abyad, Syria (van der Plicht et al., 2011, Nieuwenhuyse, 2018a). We arbitrarily assigned reasonable age uncertainties of ±25 years to the dates of these transitions. This yields the Initial to Early Pottery Neolithic transition dated to 6675±25 BCE (base of level A9 at Tell Sabi Abyad dated between 6675 – 6620 BCE; Nieuwenhuyse, 2018a), the Early Pottery Neolithic – pre Halaf transition dated at 6635±25 BCE (base of level A1 dated between 6335 - 6225 BCE; Nieuwenhuyse, 2018a) and the pre Halaf – proto-Halaf transition dated at 6015±25 BCE (this transition occurring within level B3 dated between 6040 - 5995 BCE; Nieuwenhuyse, 2018a). Note that, following Nieuwenhuyse et al. (2010), the beginning of the Initial Pottery Neolithic was placed at 7000 BCE without making a rough estimate (unnecessary for our purpose) of the uncertainties on this date. The same age uncertainties of ±25 years were also optimistically assigned to the proto-Halaf - Early Halaf, Early - Middle Halaf and Middle - Late Halaf transitions (5900±25 BCE, 5750±25 BCE, 5575±25 BCE, respectively; Bernbeck and Nieuwensuyse, 2013; Molist et al., 2013; Gómez-Bach et al., 2018; Gómez-Bach and Cruells, 2018). The case of the Late Halaf to HUT transition is different because the HUT phase remains archeologically very poorly constrained (Campbell, 2007; Campbell and Fletcher, 2010; see further discussion in Nieuwenhuyse et al., 2016 and Gómez-Bach et al., 2016). For this reason, its age uncertainties were arbitrarily increased to ±75 years, with a date at 5350±75 BCE. The time interval allowed for this transition (5425 – 5275 BCE) appears reasonable in light of current archeological uncertainties (Campbell, 2007; O. Nieuwenhuyse, personal communication). The end of HUT is just as loosely established. According to Campbell (2007), it could be dated between 5200 and 5000 BCE. A dating of 5100±100 BCE is thus roughly considered. More generally, the overall chronological framework above, which is necessarily based on some approximations and arbitrary choices (some of which are probably rather optimistic), seems to us to reasonably reflect the current state of knowledge, although other interpretations are possible.

The following age intervals were thus considered for the AH-RJMCMC calculations, with the overlaps between them being treated by the algorithm through the time order relationships:

+ Initial Pottery Neolithic (ceramic phase I at Tell Halula): 7000 - 6650 BCE

+ Early Pottery Neolithic (ceramic phase II at Tell Halula): 6700 - 6310 BCE

+ Pre Halaf (ceramic phase III at Tell Halula): 6360 - 5990 BCE

+ Proto-Halaf (ceramic phase IV at Tell Halula): 6040 - 5875 BCE

+ Early Halaf (ceramic phase V at Tell Halula): 5925 - 5725 BCE

+ Middle Halaf (ceramic phase VI at Tell Halula): 5775 - 5550 BCE

+ Late Halaf (ceramic phase VII at Tell Halula): 5600 - 5275 BCE

+ HUT: 5425 - 5000 BCE

The data obtained at Yarim Tepe I are archeologically dated to the archaic Hassuna and standard Hassuna periods, which thus involves a different terminology from that with the pre-Halaf, proto-Halaf and Halaf. Here we use a correlation scheme close to that proposed by Bernbeck and Nieuwenhuyse (2013), but with a wide age interval between 6300 and 5800 BCE without approximation made for the dating of the transition between the archaic and standard Hassuna, and with the possibility that part of the standard Hassuna defined in Iraq overlaps with part of the Early Halaf defined further east (Yutsis-Akimova et al., 2018b; O. Nieuwenhuyse, personal communication).

The results of the AH-RJMCMC modeling are shown in Fig. 2a (all data were transferred to the latitude of Tell Halaf, Syria; Tables S1, S3). Instead of showing the individual data according to their prior values, it is the posterior values (median ages and intensities with the 95% credible interval) that are exhibited (Fig. S3 shows the data using both their prior and posterior age values). This figure underlines that despite the long duration of the age intervals considered for most of the data, the time-order relationships existing between them lead to a coherent evolution of the geomagnetic intensities during the 7th and 6th millennia BCE. This evolution is marked by a steady decreasing trend during the 7th millennium, until ~6200 BCE, while it is more complex around the middle of the 6th millennium BCE, with a sharp minimum around 35 μT leading to an intensity peak between ~5600 BCE and ~5400 BCE (maximum around 5530 BCE). The maximum rates of change associated with this intensity peak are of ~0.37 μT/year (Fig. 2b; Table S3), slightly higher than those determined for the Balkans. It should be noted that the 95% credible interval during these periods remains wide, especially during the first half of the 7th millennium BCE where data are still scarce (note that these are the oldest archeointensity data obtained so far from ceramics). On the other hand, the period between ~6200 BCE and ~5600 BCE, i.e. between the end of the pre-Halaf and the middle Halaf (with data obtained at Tell Halula, Yarim Tepe II and Yarim Tepe I), seems to be characterized by the lack of significant intensity variations, as well as during the last three centuries of the 6th millennium BCE, the latter period being also marked by the lowest geomagnetic intensities over the entire 2000-year interval analyzed. It is worth pointing out that similar inferences are obtained if the time order relationship considered for the Yarim Tepe II and Yarim Tepe I data is not between the nine and eight different archeological levels as before, but between respectively 14 and 7 successive non-overlapping stratigraphic layers (still regardless of their thicknesses; Fig. S4a,b; Tables S1, S3). In this case, the data obtained in overlapping stratigraphic layers are grouped in a same layer without time order (see Table 1 in Yutsis-Akimova et al., 2018a,b).

As previously mentioned, the Late Neolithic archeological chronologies established in different areas of Mesopotamia are difficult to synchronize with each other. For this reason, we tested at first order the robustness of the curves shown in Fig. 2 by ignoring in a second calculation the age and stratigraphic position of the Middle - Late Halaf and Late Halaf - HUT transitions inside the Yarim Tepe II sequence. This amounts to considering that the Yarim Tepe II data lie in a single large time interval between ~5800 and ~5000 BCE, which therefore puts fewer constraints on correlation with data obtained further west, in Tell Halula and Tell Masaikh (Table S1). The AH-RJMCMC results presented in Fig. S4c,d show the same intensity evolution as in Fig. 2, although the amplitude of the variations is significantly smaller around 5600-5400 BCE (Table S3). The rates of change associated with the peak around 5500 BCE are also lower (maximum of ~0.17 μT/year), highlighting the sensitivity of this parameter to archeological determinations or assumptions.

4. A master Upper Mesopotamian archeointensity variation curve for the Pottery Neolithic

The regional geomagnetic field intensity models obtained for the Balkans and Upper Mesopotamia show the same peak in intensity around the middle of the 6th millennium BCE, with similar rates of change. This underlines, at least for this period, a good homogeneity of the secular variation of intensity in a large area between Bulgaria and the Near East (with a distance of ~1600 km between Sofia, Bulgaria, and the archeological site of Tell Halaf in Syria). However, two main differences are observed. The first concerns the intensity peak observed around 5800 BCE in the Balkans but not in the Near East. This age corresponds to the Early Halaf (e.g. Molist et al, 2013; Bernbeck and Nieuwenhuyse, 2013), for which a single archeointensity result was obtained at Tell Halula (Gallet et al., 2015), while there is a question as to whether the recent part of the so-called standard Hassuna period (with data obtained at Yarim Tepe I) could extend to the beginning of the Early Halaf (Yutsis-Akimova et al., 2018b; O. Nieuwenhuyse, personal communication). The second difference is in the behavior of the geomagnetic field at the end of the 6th millennium BCE, marked by an increase in intensities in the Balkans while they are fairly constant in the Near East. It is worth remarking that these two differences occur when comparing the median posterior models, it does not mean that the datasets are themselves mutually incompatible. It remains important to test whether the data obtained independently in the Balkans and in the Near East can produce a coherent evolution of geomagnetic intensities throughout the 6th millennium BCE, integrating the characteristics mentioned above. In other words, this amounts to determining what would be the influence, or implication, of the data available in the Balkans on the pattern of intensity variations in Upper Mesopotamia, assuming that the two regions shared the same secular variation in intensity during this time interval. Such a reconciliation between these two datasets might be achieved by virtue of the uncertainty in both intensity and ages, allowing the posterior distribution to effectively shift the data in both intensity and time (within their given prior distributions) to a mutually favorable configuration, in which all data are compatible with a single intensity variation curve.

A master intensity variation curve was determined for Upper Mesopotamia by transferring all Balkan data to the latitude of Tell Halaf (the Near-Eastern data used for Fig. 2a remaining unchanged). However, given the rather large distance between Bulgaria and northern Syria, this transfer carried out using the hypothesis of a simple geocentric axial dipole raises uncertainties. These are illustrated by a simple calculation: the intensity determined in Sofia from the most recent IGRF (Alken et al., 2021) is 47.9 μT; its transfer to the latitude of Tell Halaf using the same hypothesis gives 44.7 μT, to be compared to 47.6 μT determined at Tell Halaf from the IGRF. The difference of ~3 μT corresponds to ~7% of the "true" value, which is far from negligible. In order to take into account this discrepancy at first order, without of course knowing its evolution over the past millennia, we arbitrarily considered that the experimental errors on the Balkan intensity values transferred to the Near East could not be less than 3 μT (same approach as before). On the other hand, we note that the intensity variation curve derived from the Balkan data transferred to the latitude of Tell Halaf might indicate a shift in intensity around 5700-5400 BCE with respect to the Near-Eastern curve (Fig. S3). If significant, the origin of this offset would remain unclear. A possible bias due to the effect of cooling rate on thermoremanent magnetization acquisition (see discussion for example in Genevey et al., 2008) could be suggested for the Balkan data, however, this effect was considered essentially negligible for the entire dataset (Fanjat et al., 2013; Kovacheva et al., 2014; Kostadinova et al., 2019).

Furthermore, to account very roughly for the fact that the signature of the non-dipole component of the geomagnetic field may have drifted slightly from east to west, or from west to east between the Balkans and the Near East during the 6th millennium BCE, we arbitrarily considered that the dating of the Balkan data could not be more accurate than ±75 years (Table S1). This appears all the more justified since the Balkan curve transferred to the latitude of Tell Halaf also seems to present around 5700-5400 BCE a time delay of ~50 years with respect to the Near-Eastern curve (Fig. S3). However, given the data currently available and the error bars of the models, it seems premature to consider a phenomenon of eastward drift of the secular variation at this period and to shift the age of the Balkan data as a whole by ~50 years. By increasing the age uncertainties of the Balkan data, this offset, if significant, should be accounted for in the AH-RJMCMC calculations.

There are now two ways we can combine the two datasets. We could calculate the posterior distribution from only the Balkan dataset and use it as a prior to calculate the posterior distribution from the Upper Mesopotamian dataset. Alternatively, we can combine the two datasets and discover the posterior in a single calculation from this super-set. We adopt the latter strategy as it is computationally much simpler and accordingly a database of 108 data was compiled to trace the geomagnetic field intensity evolution in Upper Mesopotamia (Table S1). Below, we focus only on the 6th millennium BCE.

This master curve is shown in Fig. 3a (Table S3). As in Fig. 2a, the data are reported using their median posterior age and intensity values and the associated 95% credible interval (see details of the different symbols in the figure caption). The median intensity curve (in blue) shows a regular evolution on the multi-century time scale, which is however associated with a rather wide 95% credible interval (shaded area). This evolution now integrates the intensity peak around 5800 BCE (maximum at ~5810 BCE) seen from the Balkan data, whereas the plateau previously mentioned during the Middle Halaf is strongly attenuated (Fig. 2a). Unsurprisingly an intensity peak is clearly observed around 5550 BCE (date of the maximum). A major change concerns the end of the 6th millennium BCE where the medians of the posterior age values obtained for the HUT data are all concentrated around 5300 BCE, allowing the increase in geomagnetic intensities observed from the Balkan data.

The implications of the Balkan data on the master Upper Mesopotamian curve are also illustrated by the posterior probability distributions of median ages for some archeointensity data (Fig. 4; data indicated by open symbols in Fig. 3a). For the only result of the Early Halaf obtained at Tell Halula (SY91, Fig. 4a), it can be seen that the posterior age is mainly concentrated at both sides of the prior age interval, which leaves some room (in terms of probability) for a peak of intensity lasting about a century towards the middle of this archeological period. Moreover, two HUT results obtained at Tell Masaikh (SY37, Fig. 4b) and Yarim Tepe II (YT01, Fig. 4c) show that the posterior probability distribution of their age values is strongly concentrated in the older part of their prior age interval, suggesting that only a small part of the HUT (i.e. the oldest part) was sampled in the two sites (and see below). Such a possibility had already been raised by Yutsis-Akimova et al (2018a), but only on a purely empirical basis.

With respect to the rates of intensity change, combining the Balkan and Near-East data in the calculation yields maximum values of ~0.21 μT/year for the peak around 5800 BCE, similar to those previously obtained from the Balkan data alone (Fig. 1b). Conversely, the maximum rates of change are higher (~0.50 μT/year) for the peak around 5550 BCE, albeit with large uncertainties, than when considering the Balkan and Near East data separately. At this stage, it is unclear whether these values are relevant from a geomagnetic point of view given the approximations that have been made to combine together the Near East and Balkan data. In any case, the variation rates associated with the peak around 5550 BCE appear to be at least ~0.2 μT/year, about twice the maximum rate observed in the modern geomagnetic field (Alken et al., 2021).

5. Concluding remarks on the archeological inferences

Although Near-Eastern archeointensity datasets are still limited for the Late Neolithic, the use of the AH-RJMCMC method is already shedding light on archeological issues, whose resolution remains largely in the realm of archeology. The new insights can be summarized as follows:

• The Upper Mesopotamian data available for the Early Halaf are currently too sparse to reliably trace the geomagnetic field intensity variations during this period. Confirmation in Upper Mesopotamia of the intensity peak around 5800 BCE, still observed only from the Balkan data, would provide a crucial chronological marker, all the more important as recent excavations in Iraqi Kurdistan show that, according to the ceramic typology, the Early Halaf time interval is not clearly attested in this region (Nieuwenhuyse, 2018b and personal communication). Moreover, if the standard Hassuna defined at Yarim Tepe I does indeed extend into the Early Halaf (Yutsis-Akimova et al., 2018b; see also discussion in Cruells and Nieuwenhuyse, 2004), this overlap should not extend beyond the beginning of the Early Halaf defined further east.

• According to the Balkan results, all the archeointensity data obtained so far in Upper Mesopotamia for the Halaf-Ubaid Transitional could be dated to the beginning of this archeological phase, whose transition with the Late Halaf, defined from subtle changes in the typology and decoration of ceramics, is currently poorly circumscribed (e.g. Campbell, 2007; Nieuwenhuyse, 2018b and references therein). From the archeomagnetic point of view, the alternatives are the following: either the sampled HUT actually corresponds to the Late Halaf, or only the very beginning of the HUT is represented at Tell Masaikh and Yarim Tepe II, or the HUT was shorter than expected and does not span the last two centuries of the 6th millennium BCE (occurring between ~5400 and ~5200 BCE). It should also be noted that, at this stage, the available data are insufficient to test whether the HUT could have had a different duration between the east and west of Upper Mesopotamia. These various options echo the large archeological uncertainties still existing on the HUT phase.

• A close examination of Figs. 2 and S4 indicates that part of the Late Halaf present at Tell Halula, at ~5500-5450 BCE (see blue dots intercalated between red dots), might be absent at Yarim Tepe II, suggesting a short hiatus in the latter sequence, while the end of the Late Halaf may be absent in Tell Halula. At this stage, such a possibility is statistically far from proven, but it might be further analyzed in light of the comparative changes in ceramic typology between the two sequences. In addition, it seems conceivable that the very thin thickness (~20 cm) of archeological level VII at Yarim Tepe II, compared to the thicknesses of the other levels, is the result of low accumulation rates, perhaps a short hiatus, around the Middle to Late Halaf transition, which an age model constructed primarily from the thicknesses of the archeological levels and layers, in contrast to our AHRJMCMC age model, tends to minimize due to lack of sufficient dating constraints (see Figs. 7 and 8 in Yutsis-Akimova et al., 2018a).

In conclusion, the rapid variations in geomagnetic field intensities during the 6th millennium BCE as determined by the AH-RJMCMC method offer promising constraints for the correlation of archeological sequences established from widely distributed settlements in the Near East. In particular, these variations could help to synchronize the pottery horizons and/or archeological layers discovered in Upper Mesopotamia (Turkey, Syria, Iraq), the Levant and in the Zagros (Iran) region (e.g. Akkermans and Schwartz, 2003; Nieuwenhuyse et al., 2013; Gómez-Bach et al., 2018a).

Acknowledgements

This study is dedicated to the memory of Olivier Nieuwenhuyse. YG is very grateful to him for the very enriching discussions and helpful advise, unfortunately interrupted far too early. He also provided the pottery fragments from Tell Begum. YG thanks Miquel Molist and Shahrmardan Amirov who made possible archeointensity data acquisition in Tell Halula, Yarim Tepe II and I and for stimulating discussions. Special thanks are due to Stasya Yutsis-Akimova who analyzed the potsherds from Yarim Tepe I and II in the framework of her PhD thesis. Additional thanks are due to Anna Gómez-Bach for her comments on a preliminary version of the manuscript, and to T. Odaka for archeological information on Tell Begum. We finally thank Stuart Campbell and Javier Pavón-Carrasco for reviewing the manuscript and providing helpful comments. This is IPGP contribution no. xxxx.

References

Akkermans, P.M.M.G., Schwartz, G.M., 2003. The Archaeology of Syria. From Complex Hunter-gatherers to Early Urban Societies (ca. 16,000–300 BC). Cambridge World Archaeology, Cambridge University Press, New York, pp. 467.

Alken, P., Thébault, E., Beggan, C.D., Amit, H., Aubert, J., Baerenzung, J., Bondar, T.N., Brown, W., Califf, S., Chambodut, A., Chulliat, A., Cox, G., Finlay, C.C., Fournier, A., Gillet, N., Grayver, A., Hammer, M.D., Holschneider, M., Huder, L., Hulot, G., Jager, T., Kloss, C., Korte, M., Kuang, W., Kuvshinov, A., Langlais, B., Léger, J.M., Lesur, V., Livermore, P.W., Lowes, F.J., Macmillan, S., Magnes, W., Mandea, M., Marsal, S., Matzka, J., Metman, M.C., Minami, T., Morschhauser, A., Mound, J.E., Nair, M., Nakano, S., Olsen, N., Pavón-Carrasco, F.J., Petrov, V.G., Ropp, G., Rother, M., Sabaka, T.J., Sanchez, S., Saturnino, D., Schnepf, N.R., Shen, X., Stolle, C., Tangborn, A., Toffner-Clausen, L., Toh, H., Torta, J.M., Varner, J., Vervelidou, F., Vigneron, P., Wardinski, I., Wicht, J., Woods, A., Yang, Y., Zeren, Z., Zhou, B., 2021. International Geomagnetic Reference Field: the thirteenth generation. Earth Planets Space 73, 49.

Amirov, S., 1994. The morphology of Halafian culture ceramics based on the material collected from the settlement Yarim Tepe II (In Russian). Doctoral thesis, Moscow., pp. 144.

Amirov, S., 2018. The morphology of Halafian painted pottery from Yarim Tepe II, and the process of Ubaidian acculturation. In: Workshop on Late Neolithic ceramics in Ancient Mesopotamia in context, A. Gómez-Bach, J. Becker and M. Molist (eds.), Monografies del MAC 1, Barcelona, 13-21.

Bader, N., 1989. Earliest cultivators in Northern Mesopotamia. The Investigations of Soviet Archaeological Expedition in Iraq at Settlements Tell Magzaliya, Tell Sotto, and Kül Tepe. Moscow, Nauka.

Bashilov, V.A., Bolshakov, O.G., Kouza, A.V., 1980. The earliest strata of Yarim Tepe I. Sumer 36, 43-64.

Bernbeck, J., Nieuwenhuyse, O.P., 2013. Established paradigms, current disputes and emerging themes: the state of research on the Late Neolithic in Upper Mesopotamia. In: Interpreting the Late Neolithic of Upper Mesopotamia. Publications on Archaeology of the Leiden Museum of Archaeology (PALMA), Brepols pub. (Turnhout, Belgium), pp. 17–37.

Campbell, S., 2007. Rethinking Halaf chronology. Paléorient 33, 103-136.

Campbell, S., Fletcher, A., 2010. Questioning the Halaf-Ubaid transition. In: Carter, R.A., Philip, G. (Eds.), Beyond the Ubaid: Transformation and Integration in the Late Prehistoric Societies of the Middle East, SAOC: Studies in Ancient Oriental Civilization 63. The Oriental Institute of the University of Chicago, pp. 69–83.

Cruells, W., Nieuwenhuyse, O., 2004. The Proto-Halaf period in Syria. New sites, new data. Paléorient 30, 47-68.

Davidson, T.E; McKerrell, H., 1980. The Neutron Activation Analysis of Halaf and Ubaid Pottery from Tell Arpachiyah and Tepe Gawra, Iraq 42, 155-167.

Davidson, T.E., 1981. Pottery Manufacture and Trade at the Prehistoric Site of Tell Aqab, Syria. Journal of Field Archaeology 8, 65-77

Fanjat, G., Aidona, E., Kondopoulou, D., Camps, P., Rathossic C., Poidras T., 2013. Archeointensities in Greece during the Neolithic period: New insights into material selection and secular variation curve. Phys. Earth Planet. Inter. 215, 29-42.

Forest, J.-D., 2013. The birth of a new culture: at the origin of the Halaf. In: Interpreting the Late Neolithic of Upper Mesopotamia. Publications on Archaeology of the Leiden Museum of Archaeology (PALMA), Brepols pub. (Turnhout, Belgium), pp. 101-105.

Frangipane, M., 2013. Societies without boundaries: interpreting Late Neolithic patterns of wide interaction and sharing of cultural traits. The case of the Halaf communities. In:

Interpreting the Late Neolithic of Upper Mesopotamia. Publications on Archaeology of the Leiden Museum of Archaeology (PALMA), Brepols pub. (Turnhout, Belgium), pp. 89–99.

Gallet, Y., Le Goff, M., 2006. High-temperature archeointensity measurements from Mesopotamia. Earth Planet. Sci. Lett. 241, 159-173.

Gallet, Y., Genevey, A., Le Goff, M., Warmé, N., Gran−Aymerich, J., Lefèvre, A., 2009. On the use of archeology in geomagnetism, and vice−versa: Recent developments in archeomagnetism, C. R. Physique 10, 630−648.

Gallet, Y., Molist, M., Genevey, A., Clop Garcia, X., Thébault, E. Gómez Bach, A., Le Goff, M. Robert, B., Nachasova, I., 2015. New Late Neolithic (c. 7000-5000 BC) archeointensity data from Syria. Reconstructing 9000 years of archeomagnetic field intensity variations in the Middle East. Phys. Earth Planet. Inter. 238, 89-103.

Gallet, Y., Fortin, M., Fournier, A., Le Goff, M., Livermore, P., 2020. Analysis of geomagnetic field intensity variations in Mesopotamia during the third millennium BC with archeological implications. Earth Planet. Sci. Lett. 537, 116183.

Genevey, A., Gallet, Y., Constable, C.G., Korte, M., Hulot, G., 2008. ArcheoInt: an up-graded compilation of geomagnetic field intensity data for the past ten millennia and its application to the recovery of the past dipole moment. Geochem. Geophys. Geosyst. 9, Q04038

Genevey, A., Gallet, Y., Thébault, E., Livermore P.W., Fournier, A., Jesset, S., Lefèvre, A., Mahé-Hourlier, N., Marot, E., Regnard S., 2021. Archeomagnetic intensity investigations of French Medieval ceramic workshops: Contribution to regional field modeling and archeointensity-based dating. Phys. Earth Planet. Inter. 318, 106750.

Gómez-Bach, A., Cruells, W., Molist, M., 2016. Sharing spheres of interaction in the 6th millennium cal. BC: Halaf communities and beyond. Paléorient 42, 117-133.

Gómez-Bach, A., Cruells, W., 2018. Time and technological transfer in proto-Halaf and Halaf sequences at Chagar Bazar (Khabur valley, Syria). In: Workshop on Late Neolithic ceramics in Ancient Mesopotamia in context, A. Gómez-Bach, J. Becker and M. Molist (eds.), Monografies del MAC 1, Barcelona, 67-82.

Gómez-Bach, A., Becker, J., Molist, M. (eds.), 2018a. Workshop on Late Neolithic ceramics in Ancient Mesopotamia in context, Monografies del MAC 1, Barcelona, 45-57.

Gómez-Bach, A., Cruells, W., Molist, 2018b. Halaf phenomena: surplus, homeland and identity in Upper Mesopotamia (6.200-5.300 cal BC). In: Herusgeber, H.M.; Detlef, G.; Risch, R., Surplus without the State. Political Forms in Prehistory. 10. Mitteldeutscher Archäologentag, vom 19 bis 21 Oktober 2017 in Hale (Saale), Tagungen des Landesmuseums für Vorgeschichte Halle, Band 18, 147-166.

Gómez-Bach, A., Clop, X., Molist, M., 2018c. Red ware: characterizing a pottery production at Tell Halula at mid-sixth millennium cal BC. In: Workshop on Late Neolithic ceramics in Ancient Mesopotamia in context, A. Gómez-Bach, J. Becker and M. Molist (eds.), Monografies del MAC 1, Barcelona, 141-147.

Hervé, G., Lanos, P., 2017. Improvements in Archaeomagnetic Dating in Western Europe from the Late Bronze to the Late Iron Ages: An Alternative to the Problem of the Hallstattian Radiocarbon Plateau: Improvements in archaeomagnetic dating in Western Europe. Archaeometry 60 (4), 870-883.

Hole, F., 2013. Constrained innovation: Halafian ceramics. In: Interpreting the Late Neolithic of Upper Mesopotamia. Publications on Archaeology of the Leiden Museum of Archaeology (PALMA), Brepols pub. (Turnhout, Belgium), pp. 77–87.

Huot, J.-L., 2004. Une archéologie des peuples du Proche-Orient I. Des premiers villageois aux peuples des cités-états. Editions Errance, Paris, pp. 249.

Korte, M., Brown, M., Gunnarson, S.R., Nilsson, A., Panovska, S., Wardininski, I., Constable C.G., 2019. Refinig Holocene geochronologies using paleomagnetic records. Quaternay Geochronology 50, 47-74.

Kostadinov-Avramova, M., Kovacheva, M., Boyadzhiev, Y., Hervé, G., 2019. Archaeomagnetic knowledge of the Neolithic in Bulgaria with emphasis on intensity changes. Geol. Soc. Lond., Spec. Publ. 497.

Kovacheva, M., Kostadinova-Avramova, M., Jordanova, N., Lanos, P., Boyadziev, Y., 2014. Extended and revised archaeomagnetic database and secular variation curves from Bulgaria for the last eight millennia. Phys. Earth Planet. Inter. 236, 79-94.

Lanos, P., 2004. Bayesian inference of calibration curves: application to archaeomagnetism, in: Tools for Constructing Chronologies. Springer, pp. 43-82.

Le Goff, M., Gallet, Y., Genevey, A., Warmé, N., 2002. On archaeomagnetic secular variation curves and archaeomagnetic dating. Phys. Earth Planet. Inter. 134, 203–211.

Le Goff, M., Gallet, Y., 2004. A new three-axis vibrating sample magnetometer for continuous high-temperature magnetization measurements: applications to paleo- and archeo-intensity determinations. Earth Planet. Sci. Lett. 229, 31-43.

Livermore, P.W., Fournier, A., Gallet, Y., Bodin, T., 2018. Transdimensional inference of archeomagnetic intensity change. Geophys. J. Int. 215, 2008-2034.

Livermore, P.W., Gallet, Y., Fournier, A., 2021. Archeomagnetic intensity variations during the era of geomagnetic spikes in the Levant. Phys. Earth Planet. Inter. 312, 106657.

Merpert, N.J., Munchaev, R.M., 1987. The Earliest Levels at Yarim Tepe I and Yarim Tepe II in Northern Iraq. Iraq 49, 1-36.

Merpert, N.J., Munchaev, R.M. 1993a. Yarim Tepe I. In: Early stages in the evolution of Mesopotamian civilizations: Soviet excavations in Northern Iraq, N. Yoffee and J. Clark (Ed.), pp. 73-114. Tucson: University of Arizona Press.

Merpert, N.J., Munchaev, R.M. 1993b. Yarim Tepe II: The Halaf levels. In: Early stages in the evolution of Mesopotamian civilizations: Soviet excavations in Northern Iraq, N. Yoffee and J. Clark (Ed.), pp. 129-162. Tucson: University of Arizona Press.

Molist, M., Anfruns, J., Bofill, M., Borrell, F., Buxy, R., Clop, X., Cruells, W., Faura, J.M., Ferrer, A., Gómez, A., Guerrero, E., Saca, M., Tornero, C., Vicente, O., 2013. Tell Halula (Euphrates Valley, Syria): New approach to VII and VI millennia cal. B.C. in Northern Levant framework. In: Interpreting the Late Neolithic of Upper Mesopotamia. Publications on Archaeology of the Leiden Museum of Archaeology (PALMA), Brepols pub. (Turnhout, Belgium), pp. 443–455.

Nieuwenhuyse, O., Akkermans, P., van der Plicht, J., 2010. Not so coarse, nor always plain - the earliest pottery of Syria. Antiquity 84, 71-85.

Nieuwenhuyse, O.P., Bernbeck, R., Akkermans, P.M.M.G., Rogasch, J., 2013. Interpreting the Late Neolithic of Upper Mesopotamia. Publications on Archaeology of the Leiden Museum of Archaeology (PALMA), Brepols pub. (Turnhout, Belgium), pp. 520.

Nieuwenhuyse, O., 2013. The social uses of decorated ceramics in Late Neolithic Upper Mesopotamia. In: Interpreting the Late Neolithic of Upper Mesopotamia. Publications on Archaeology of the Leiden Museum of Archaeology (PALMA), Brepols pub. (Turnhout, Belgium), pp. 135–145.

Nieuwenhuyse, O., Odaka, T., Kaneda, A., Mühl, S., Rasheed, K., Altaweel, M., 2016. Revisiting Tell Begum: a prehistoric site in the Shahrizor plain, Iraqi Kurdistan. Iraq 78, 103-135.

Nieuwenhuyse, O. (Ed.), 2018a. Relentlessly plain: seventh millennium ceramics at Tell Sabi Abyad, Syria. Oxbow Books, Oxford & Philadelphia, 396 p.

Nieuwenhuyse, O., 2018b. In the Shahrizor. Reassessing the Halaf ceramic traditions of Iraqi Kurdistan. In: Workshop on Late Neolithic ceramics in Ancient Mesopotamia in context, A. Gómez-Bach, J. Becker and M. Molist (eds.), Monografies del MAC 1, Barcelona, 43-55.

Odaka, T., Nieuwenhuyse, O., Mühl, S., 2019. From the 7^{th} to the 6^{th} millennium BC in Iraqi Kurdistan: a local ceramic horizon in the Shahrizor plain. Paléorient 45 (2), 67-83.

Pavón-Carrasco, F.J., Rodríguez-González, J., Osete, M. L., Torta, J. M., 2011. A MATLAB tool for archaeomagnetic dating. J. Archaeol. Sci. 38, 408-419.

Principe, C., Gogichaishvili, A., Arrighi, S., Devidze, M., La Felice, S., Paolillo, A., Giordano, D., Morales, J., 2018. Archaeomagnetic dating of Copper Age furnaces at Croce di Papa village and relations on Vesuvius and Phlegraean Fields volcanic activity. J. Volcanol. Geotherm. Res. 349, 217-229.

Robert, B., Blanc, C., Masetti-Rouault, M-G. 2008. Characterizing the Halaf-Ubaid Transitional Period by studying ceramic from Tell Masaikh, Syria. Archaeological data and archeometry investigations. In : Kühne H., Czichon R.M., Kreppner F.J. (ed.), Proceedings of 4th International Congress of the Archaeology of the Ancient Near East, Wiesbaden, Harrassowitz, 225-234

Robert, B., 2010. Développement et disparition de la production céramique halafienne: implications techniques et sociales à partir d'études de cas. PhD thesis Université Lumière Lyon 2, pp. 899.

Schnepp, E., Obenaus, M., Lanos, P., 2015. Posterior archaeomagnetic dating: An example from the Early Medieval site Thunau am Kamp, Austria. J. Archaeol. Sci. Rep. 2, 688-698.

Shaar, R., Bechar, S., Finkelstein, I., Gallet, Y., Martin, M., Ebert, Y., Keinan, J., Gonen, L.,

2020. Synchronizing geomagnetic field intensity records in the Levant between the 23rd and 15th centuries BCE: chronological and methodological implications. Geochem., Geophys., Geosyst. 21, e2020GC009251.

Spataro, M., Fletcher, A., 2010. Centralisation or regional identity in the Halaf period? Examining interactions within fine painted ware production. Paléorient, 36, 91-116.

Thellier, E., Thellier, O., 1959. Sur l'intensité du champ magnétique terrestre dans le passé historique et géologique. Ann. Géophys. 15, 285–376.

Tsuneki A., Nieuwenhuyse O., Campbell, S. (eds.), 2017. The Emergence of Pottery in West Asia. Oxford and Philadelphia: Oxbow Books. 192 pp.

Van der Plicht, J., Akkermans, P.M.M.G., Nieuwenhuyse, O., Kaneda, A., Russell, A. 2011. Tell Sabi Abyad, Syria: radiocarbon chronology, cultural change, and the 8.2 ka event. Radiocarbon 53, 229-243.

Yutsis-Akimova, S., Gallet, Y., Amirov, S., 2018a. Rapid geomagnetic field intensity variations in the Near East during the 6th millennium BC: New archeointensity data from Halafian site Yarim Tepe II (Northern Iraq). Earth Planet. Sci. Lett. 482, 201-212.

Yutsis-Akimova, S., Gallet, Y., Petrova, N., Nowak, S., Le Goff, M., 2018b. Geomagnetic field in the Near East at the beginning of the 6th millennium BC: Evidence for alternating weak and strong intensity variations. Phys. Earth Planet. Inter. 282, 49-59.

Figure captions

Fig. 1. (a) Evolution of the geomagnetic field intensity in the Balkans during the 6th millennium BCE estimated using the AH-RJMCMC method (Livermore et al., 2018). Blue dots and triangles: data with and without pTRM checks from Kovacheva et al. (2014); red dots: data from Kostadinova-Avramova et al. (2019); green dot: a result from Greece obtained by Fanjat et al. (2013); see text for further description. The variation curve (median values) is in blue and the light blue shaded area show its 95% credible interval. The average curve calculated by Kovacheva et al. (2014) using the Lanos (2004) method is also shown (pale orange). (b) Medians and credible interval of the intensity variation rates estimated for the Balkans using the AH-RJMCMC method. All data are transferred to the latitude of Sofia (λ=42.70°N).

Fig. 2. Same as in Fig. 1 but for the Upper Mesopotamian region during the 7th and 6th millennia BCE. Blue dots and triangles: data from Tell Halula and Tell Masaikh (Gallet et al., 2015); red dots and triangles: data from Yarim Tepe II (Yutsis-Akimova et al., 2018a) and Yarim Tepe I (Yutsis-Akimova et al., 2018b). All data are transferred to the latitude of Tell Halaf (Syria; λ=36.82°N). The archeological periodization is shown at the top of the figure. The grey zones indicate the estimated uncertainties in the age of the archeological transitions (see text).

Fig. 3. Same as in Figs. 1 and 2 but for a dataset combining the results available from the Balkans and Upper Mesopotamia. See text for changes to the Balkan archeointensity data. Same symbols and color code as before for the Upper Mesopotamian data, except for three data shown by empty symbol that are further illustrated in Fig. 4 (dot circled in blue: SY91,

Tell Halula; triangle with blue lines: SY37, Tell Masaikh; dot circled in red: YT01, Yarim Tepe II). Grey dots, triangles and square: Data from the Balkans obtained by Kovacheva et al. (2014), Kostadinova-Avramova et al. (2019) and Fanjat et al. (2013), respectively.

Fig. 4. Comparison between the joint posterior probability distributions of the median age and intensity values (green bars) and the corresponding prior values (pale orange) for three different archeointensity results. (a) Early Halaf-dated result obtained at Tell Halula (SY91; Gallet et al., 2015); (b) HUT result from Tell Masaikh (SY37; Gallet et al., 2015); (c) HUT result from Yarim Tepe II (YT01; Yutsis-Akimova et al., 2018a).

Supplementary material

Fig. S1. New archeointensity data from Tell Begum (λ=35°17'5''N, ϕ=45°53'05''E) in Iraqi Kurdistan obtained from HUT fine ware pottery. Archeological reference: Level IV, Lower Trench (LT) sounding locus 4, BEG39-40. The data were obtained using the Triaxe protocol (Le Goff and Gallet, 2004) and obey the same selection criteria as for instance in Gallet and Le Goff (2006), Gallet et al. (2015; 2020), Yutsis-Akimova et al. (2018a,b). Each curve shows the R'(Ti) data obtained for one specimen (Le Goff and Gallet, 2004), with a minimum of two, but more often three specimens successfully analyzed per fragment. Five fragments provided archeointensity results, although the presence of a secondary magnetization component in these fragments required intensity determinations at relatively high temperatures (T1' >300°C; see details in Gallet and Le Goff, 2004 and other references mentioned above).

Fig. S2. (a,c) Evolution of the geomagnetic field intensities in the Balkans during the 6th millennium BCE estimated using the AH-RJMCMC method (Livermore et al., 2018). Blue dots and triangles: data with and without pTRM checks from Kovacheva et al. (2014); red dots: data from Kostadinova-Avramova et al. (2019); green dot: a result from Greece obtained by Fanjat et al. (2013); see text for further description. The variation curve (median values) is in blue and the shaded area show its 95% credible interval. For these computations, the data that were not constrained by pTRM checks were modified so that their minimum experimental errors cannot be less than ±5.0 mT (see text). In addition the dating accuracy of all the data cannot be more accurate than ±50 years (a) and ±75 years (c). (b,d) Medians and 95% credible interval of the intensity variation rates estimated for the Balkans using the AH-RJMCMC method (with minimum age uncertainties of ± 50 years (b) and ±75 years (d)). All data are transferred to the latitude of Sofia (λ=42.70°N).

Fig. S3. Evolution of the geomagnetic field intensities in Upper Mesopotamia during the 7th and 6th millennia BCE estimated using the AH-RJMCMC method (Livermore et al., 2018). (a) The data available in the Near East are shown using their prior dating. The variation curve (median values) and its 95% credible interval are in blue. The orange curve and shaded area show the evolution of the intensities derived from the Balkan data transferred to the latitude of Tell Halaf and assigning to these data minimum age uncertainties of ±50 years. (b) Same as in (a) but the data are exhibited using the posterior probability distributions of their age values.

Fig. S4. Behavior in geomagnetic field intensity as derived from the Upper Mesopotamian data (Gallet et al., 2015; Yutsis-Akimova et al., 2018a,b; this study). All data are transferred to the latitude of Tell Halaf, Syria. (a,b) Same as in Fig. 2 but the time order relationship between the data from Yarim Tepe II concerns 14 non-overlapping stratigraphic layers, instead of nine archeological levels (see text). (c,d) Same as in Fig. 2 but the archeological transitions inside the Yarim Tepe II sequence are ignored for the AH-RJMCMC calculations (see Section 3b).

Table S1. Different datasets from the Balkans and the Near East used for AH-RJMCMC modeling (see text and details in the table).

Table S2. New archeointensity data obtained at Tell Begum. Mean intensities are first estimated at the specimen level, then at the fragment level, and finally at the fragment group level. This last group-mean value is used for the AH-RJMCMC modeling, with a dating of 5400±75 BCE (Odaka et al., 2019). T_1'-T2, Temperature interval (in °C) for intensity determination; Hlab, laboratory field used for TRM acquisition; NRM T_1' (%), fraction of NRM involved in intensity determination; Slope R' (%), slope of the R'(Ti) data within the temperature interval used for intensity determination; F, intensity value in μT derived per specimen; F mean value per fragment ± σ, mean intensity in μT computed per fragment with its standard deviation. Group F mean value ± σ, mean intensity in μT computed for each group of fragments.

Table S3. Medians and 95% credible intervals estimated using the AH-RJMCMC method (Livermore et al. 2018) and associated rates of changes (based on the time derivative of the medians) shown in Figs. 1, 2, 3, S2 and S4. The datasets are those provided in Table S1. See text

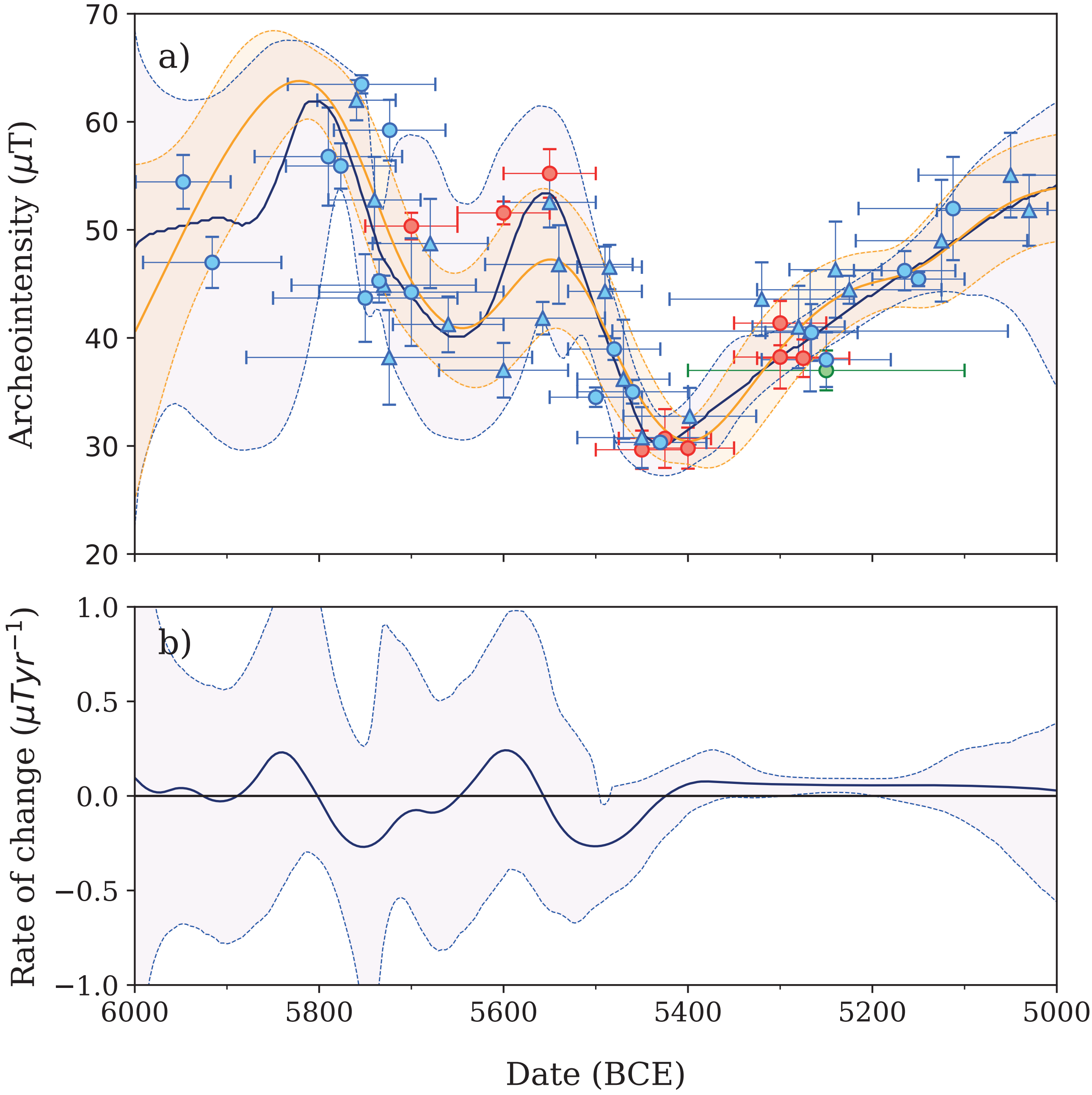
a)
b)
Archeointensity (μT)
Rate of change ($\mu T yr^{-1}$)
70
60
50
40
30
20
1.0
0.5
0.0
−0.5
−1.0
6000
5800
5600
5400
5200
5000
Date (BCE)

Figure 1

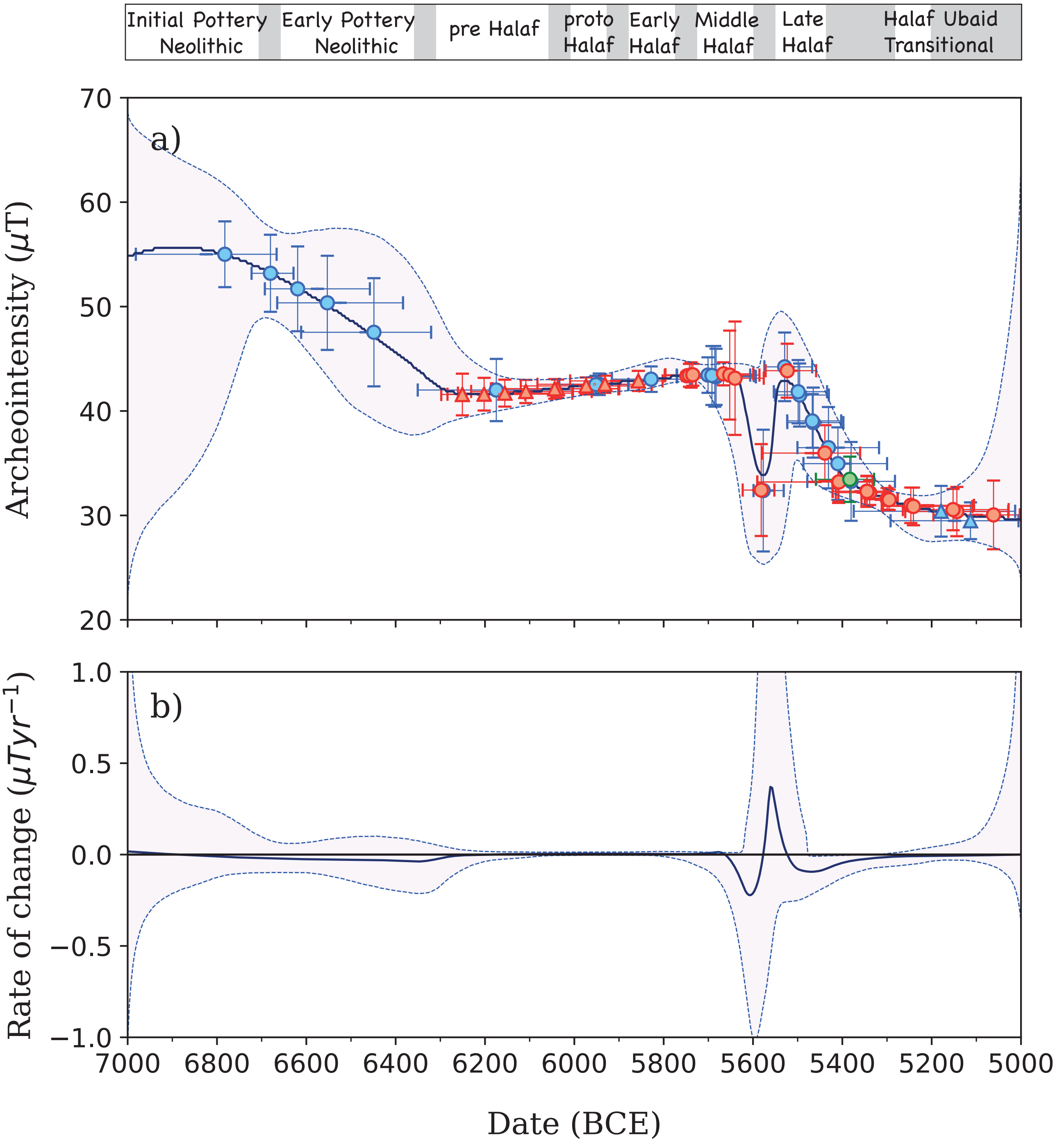

Initial Pottery Neolithic
Early Pottery Neolithic
pre Halaf
proto Halaf
Early Halaf
Middle Halaf
Late Halaf
Halaf Ubaid Transitional
a)
b)
Archeointensity (μT)
Rate of change (μTyr⁻¹)
Date (BCE)

Figure 2

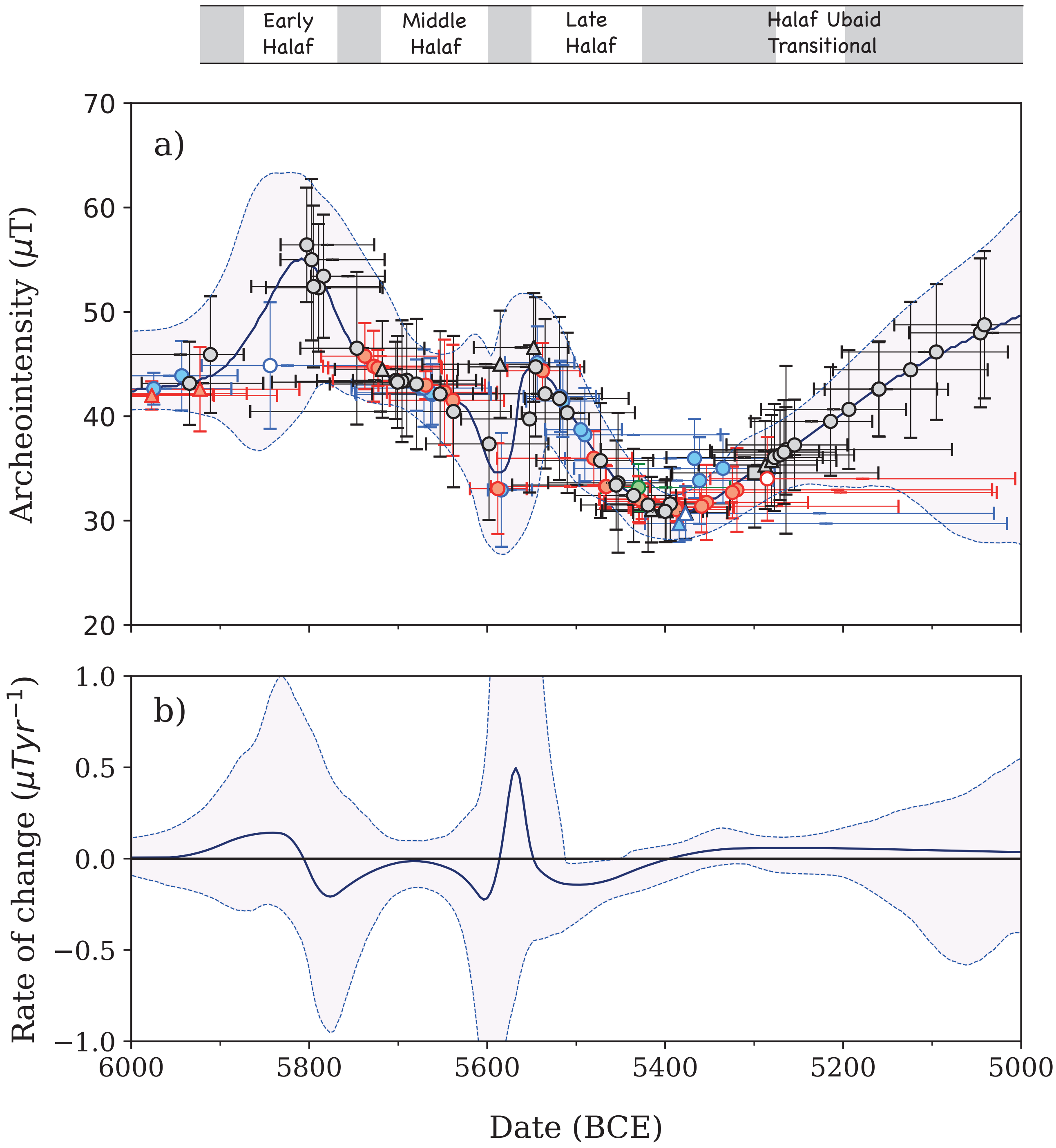

Early Halaf
Middle Halaf
Late Halaf
Halaf Ubaid Transitional
a)
b)
Archeointensity (μT)
Rate of change (μTyr⁻¹)
Date (BCE)
70
60
50
40
30
20
1.0
0.5
0.0
−0.5
−1.0
6000
5800
5600
5400
5200
5000

Figure 3

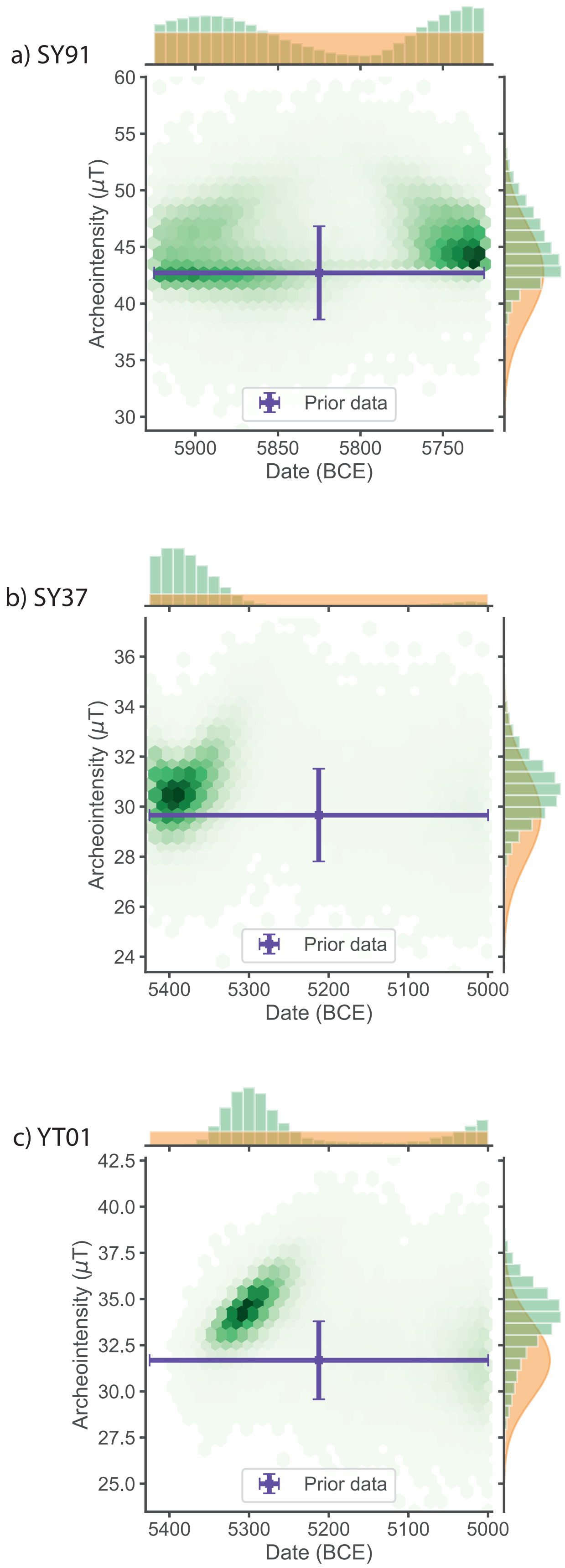

a) SY91
Archeointensity (μT)
Date (BCE)
Prior data
b) SY37
Archeointensity (μT)
Date (BCE)
Prior data
c) YT01
Archeointensity (μT)
Date (BCE)
Prior data

Figure 4

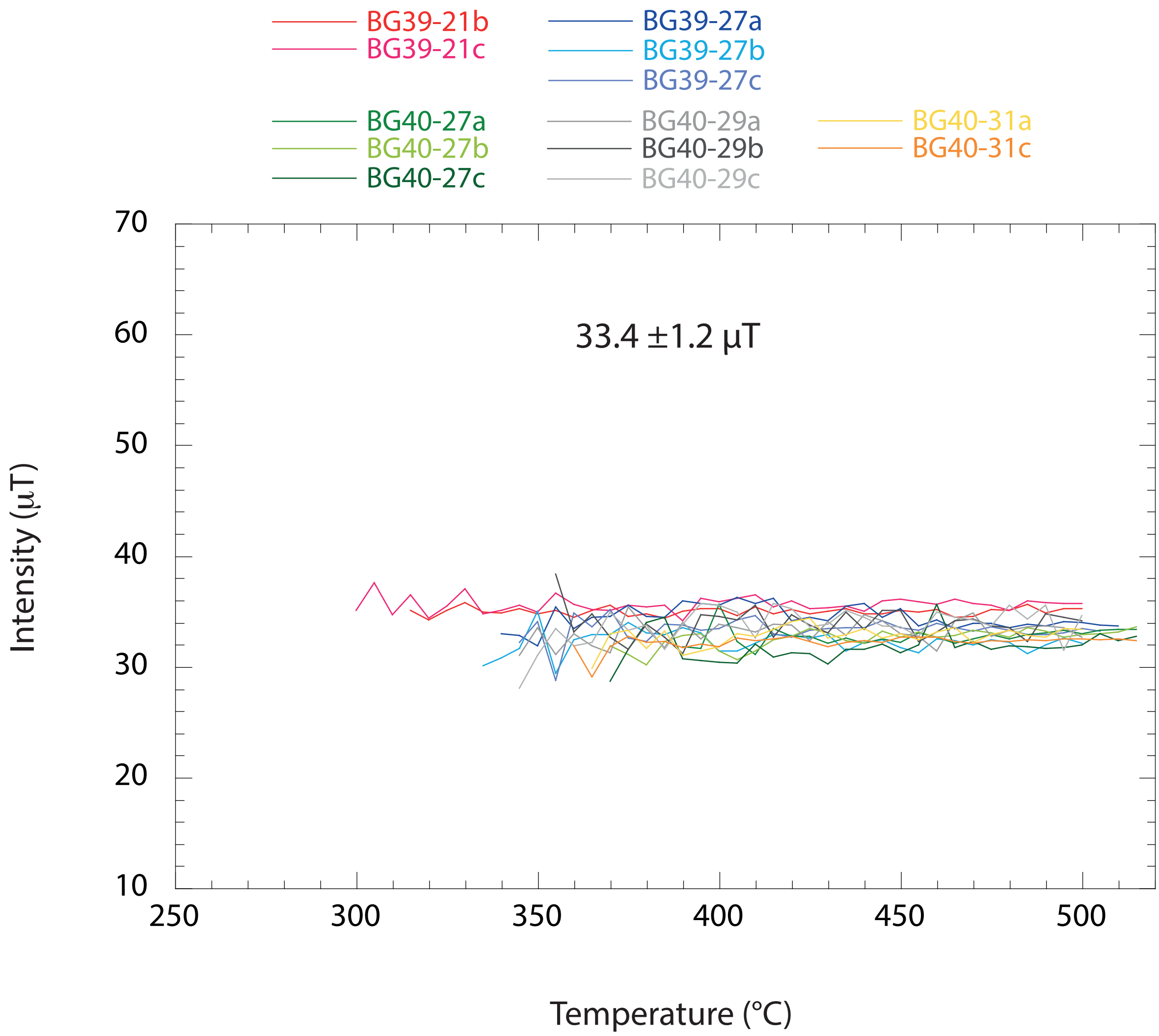
BG39-21b
BG39-21c
BG39-27a
BG39-27b
BG39-27c
BG40-27a
BG40-27b
BG40-27c
BG40-29a
BG40-29b
BG40-29c
BG40-31a
BG40-31c
70
60
50
40
30
20
10
250
300
350
400
450
500
33.4 ±1.2 µT
Intensity (µT)
Temperature (°C)

Figure S1

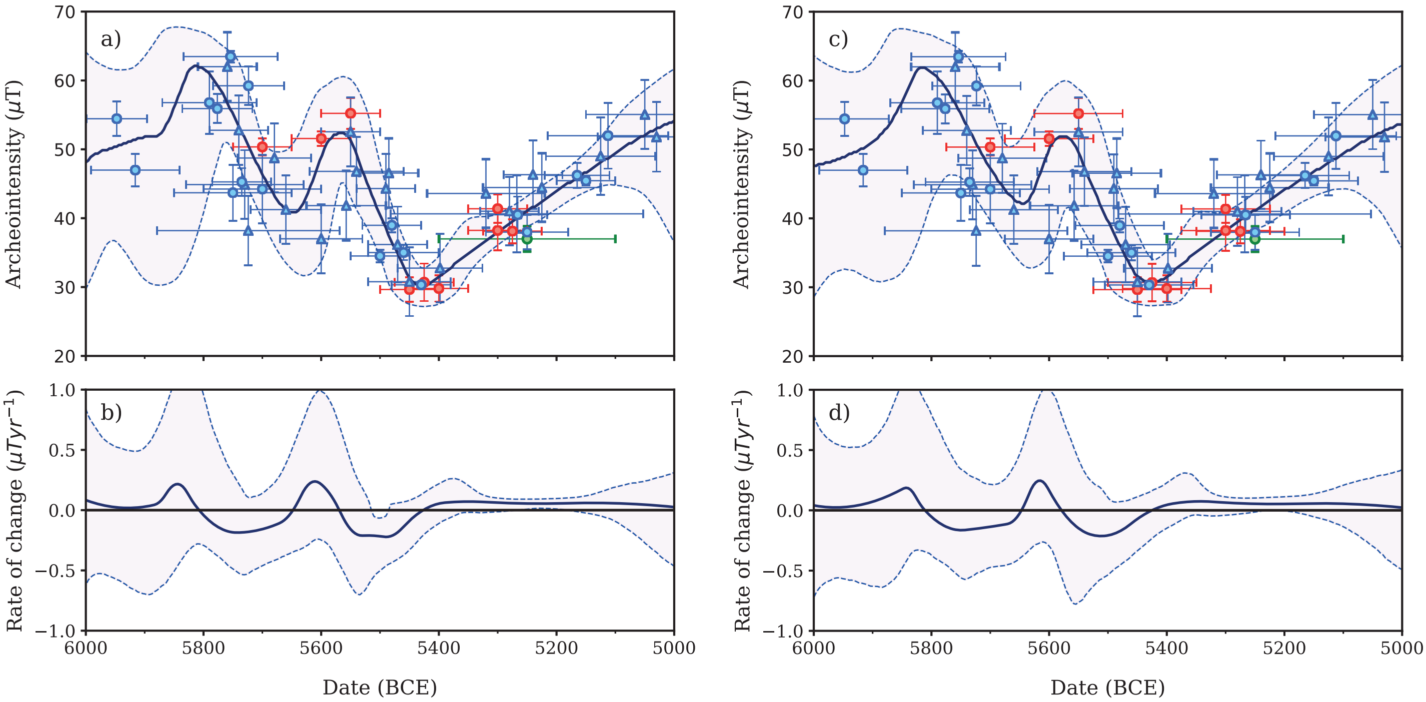
a)
b)
c)
d)
Archeointensity (μT)
Rate of change (μTyr⁻¹)
Date (BCE)
70
60
50
40
30
20
1.0
0.5
0.0
−0.5
−1.0
6000
5800
5600
5400
5200
5000

Figure S2

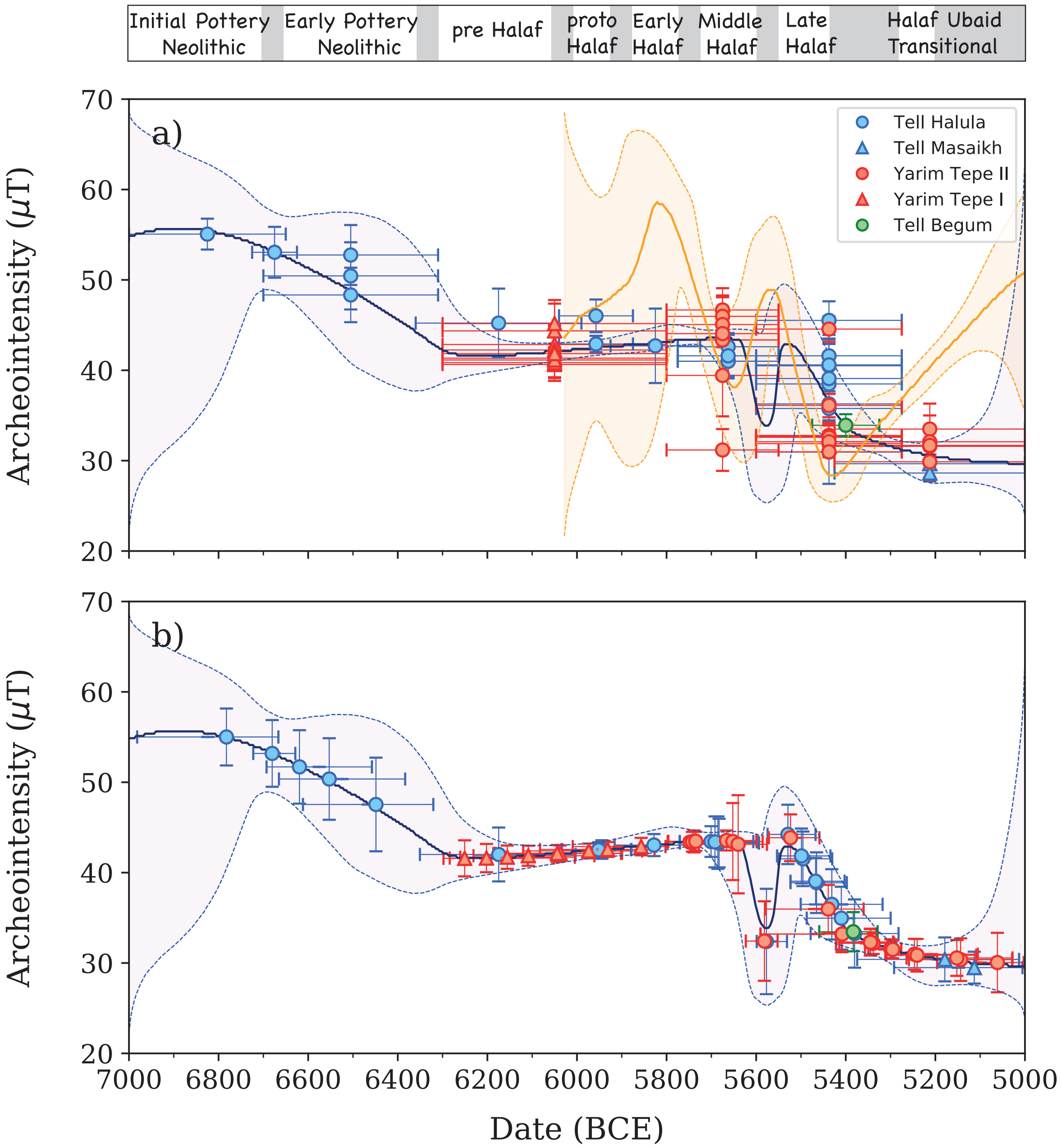
Initial Pottery Neolithic
Early Pottery Neolithic
pre Halaf
proto Halaf
Early Halaf
Middle Halaf
Late Halaf
Halaf Ubaid Transitional
a)
b)
Tell Halula
Tell Masaikh
Yarim Tepe II
Yarim Tepe I
Tell Begum
Archeointensity (μT)
Date (BCE)
70
60
50
40
30
20
7000
6800
6600
6400
6200
6000
5800
5600
5400
5200
5000

Figure S3

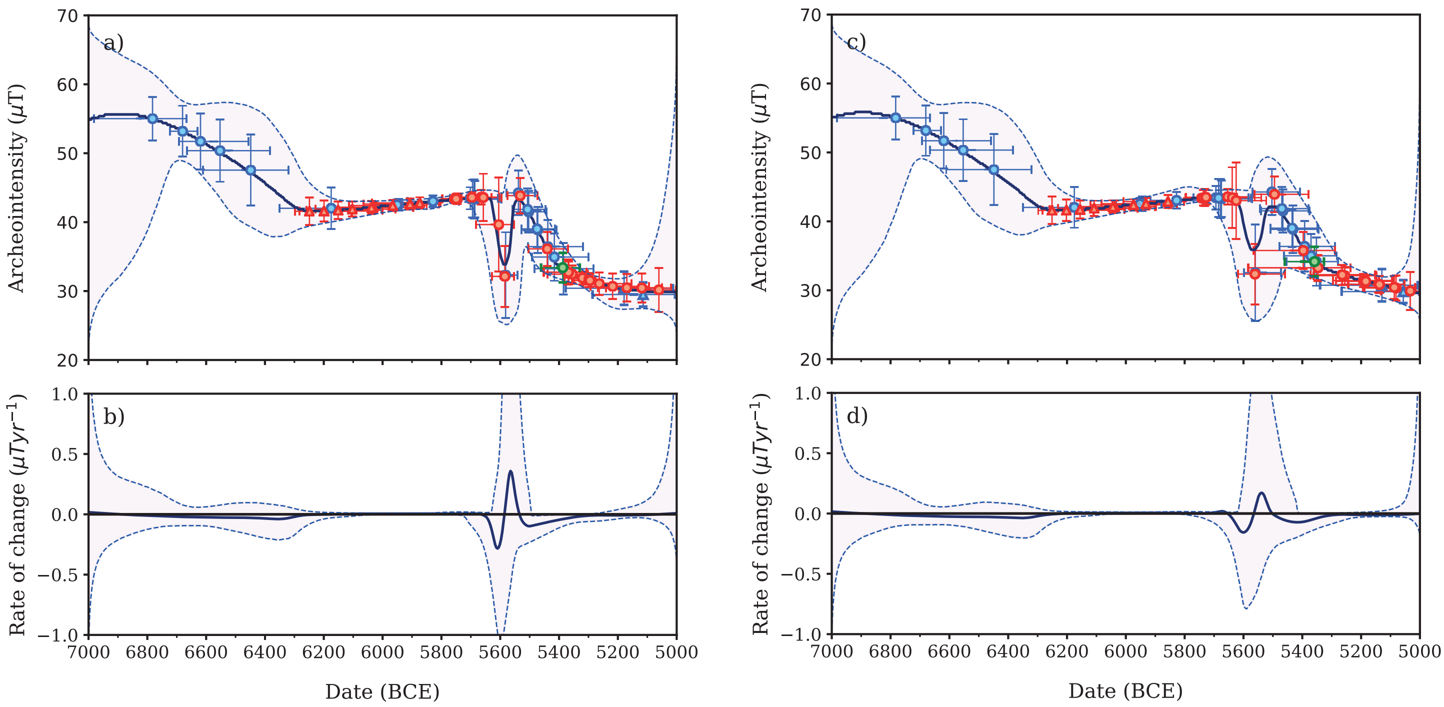
a)
b)
c)
d)
Archeointensity (μT)
Rate of change (μTyr^{-1})
Date (BCE)
70
60
50
40
30
20
1.0
0.5
0.0
−0.5
−1.0
7000
6800
6600
6400
6200
6000
5800
5600
5400
5200
5000

Figure S4

Archeol. Ref.	Fragment	Specimen	T_1'-T_2 (°C)	H_{Lab} (μT)	NRM T_1' (%)	Slope *R'* (%)	F (μT)	F mean value per fragment ± σ (μT)	Group F mean value ± σ (μT)
Level IV LT, Loc 4 Lot39-40	**BEG39-21**	BG39-21b	315 - 510	35	85	0	35.0	35.3 ± 0.4	
		BG39-21c	320 - 510	35	86	1	35.6		
	BEG39-27	BG39-27a	315 - 510	35	75	-1	34.4	33.3 ± 1.1	
		BG39-27b	315 - 510	35	75	0	32.2		
		BG39-27c	390 - 515	35	73	1	33.3		
	BEG40-27	BG40-27a	370 - 515	35	68	3	32.7	32.3 ± 0.5	
		BG40-27a	370 - 515	35	69	7	32.5		
		BG40-27a	315 - 510	35	69	5	31.7		
	BEG40-29	BG40-29a	345 - 510	35	75	4	33.1	33.6 ± 0.4	
		BG40-29b	355 - 510	35	69	-1	33.9		
		BG40-29c	345 - 510	35	69	8	33.7		
	BEG40-31	BG40-31a	365 - 510	35	72	5	32.7	32.5 ± 0.4	
		BG40-31c	360 - 510	35	75	3	32.2		
	MEAN								**33.4 ± 1.2**

Table S2